Precision lifetime measurements of Cs $6p\ ^2P_{1/2}$ and $6p\ ^2P_{3/2}$ levels by single-photon counting

L. Young,* W. T. Hill III,† S. J. Sibener,‡ Stephen D. Price,§ C. E. Tanner,‖
C. E. Wieman,¶ and Stephen R. Leone**
Joint Institute for Laboratory Astrophysics, National Institute of Standards and Technology and University of Colorado, Boulder, Colorado 80309-0440
(Received 28 March 1994)

Time-correlated single-photon counting is used to measure the lifetimes of the $6p\ ^2P_{1/2}$ and $6p\ ^2P_{3/2}$ levels in atomic Cs with accuracies $\approx 0.2-0.3\%$. A high-repetition-rate, femtosecond, self-mode-locked Ti:sapphire laser is used to excite Cs produced in a well-collimated atomic beam. The time interval between the excitation pulse and the arrival of a fluorescence photon is measured repetitively until the desired statistics are obtained. The lifetime results are 34.75(7) and 30.41(10) ns for the $6p\ ^2P_{1/2}$ and $6p\ ^2P_{3/2}$ levels, respectively. These lifetimes fall between those extracted from *ab initio* many-body perturbation-theory calculations by Blundell, Johnson, and Sapirstein [Phys. Rev. A **43**, 3407 (1991)] and V. A. Dzuba *et al.* [Phys. Lett. A **142**, 373 (1989)] and are in all cases within 0.9% of the calculated values. The measurement errors are dominated by systematic effects, and methods to alleviate these and to approach an accuracy of 0.1% are discussed. The technique is a viable alternative to the fast-beam laser approach for measuring lifetimes with extreme accuracy.

PACS number(s): 32.70.Fw, 32.70.Cs, 42.55.Rz

I. INTRODUCTION

There is renewed interest in accurate lifetime measurements of excited states in alkali-metal atoms [1,2]. The interest stems from the need to test *ab initio* theory [3,4], which is used to interpret parity nonconservation (PNC) measurements in atomic cesium [5]. Ideally, it is desirable to establish the accuracy of these many-body perturbation-theory (MBPT) calculations in heavy atoms at an $\approx 0.1-0.2\%$ level in order to eliminate the theoretical contribution [6] to the error in the extraction of the weak charge Q_w from PNC experiments in Cs atoms. The MBPT calculations can be tested by comparison with binding energies, hyperfine structure (hfs) constants, and dipole matrix elements. While experimental values for the first two quantities are far more precise than theory (theoretical errors are estimated to be 0.5%, 1%, and 0.5% for energies, hfs, and dipole matrix elements, respectively), the dipole matrix element comparison is limited by the precision of lifetime data [1,7]. This last comparison is particularly critical for the interpretation of the PNC experiments because the measurement obtains the ratio of the parity nonconserving electric dipole ($E1$) to the Stark-induced amplitude for the $6s$-$7s$ transition. Previous precision measurements of the Stark effect [8,9], which involves sums of dipole matrix elements, also provide an important test of these calculations. More generally, it would be comforting to verify the accuracy of the calculations for the behavior of the wave function both near the nucleus (hfs) and at large r (lifetimes).

The reliability of the MBPT calculations of lifetimes at the sub-1% level (dipole matrix elements) for heavy alkali-metal atoms has been cast into some doubt by the discrepancies between experiment and theory in the light alkali-metal atoms. Specifically, in Li and Na experimental lifetimes [10] for the first excited p states are $\sim 0.6\%$ and 0.9% longer than the "all-order" MBPT theoretical lifetimes [11,12]. This difference is significant since the estimated errors in Li are 0.15% experimental [10] and 0.05% theoretical [11]. However, other somewhat less precise measurements, such as the $(0.5-0.7\%)$ single-photon counting measurements [13,14], show no significant deviation ($<2\sigma$) from theory in either Li or Na, emphasizing the need for extreme experimental accuracy.

The situation in Cs is somewhat different: both experimental and theoretical lifetimes for the first excited p states are less accurate than for the lighter alkali-metal atoms. The current MBPT calculations of the $6s$-$6p$ dipole matrix element have an estimated error of $\sim 0.5\%$ [3]. However, there are credible expectations that improvements in the calculations will yield an increase in

*Permanent address: Physics Division, Argonne National Laboratory, Argonne, IL 60439.
†Permanent address: Institute for Physical Science and Technology, University of Maryland, College Park, MD 20742.
‡Permanent address: James Franck Institute, University of Chicago, Chicago, IL 60637.
§Permanent address: Department of Chemistry, University of College London, London WC1H 0AJ, England.
‖Permanent address: Department of Physics, University of Notre Dame, Notre Dame, IN 46556.
¶Also at Department of Physics, University of Colorado, Boulder, CO 80309-0440.
**Also at Quantum Physics Division, National Institute of Standards and Technology, and Departments of Chemistry and Physics, University of Colorado, Boulder, CO 80309-0440.

theoretical precision of an order of magnitude [3,15]. The two previous most precise experimental lifetimes for the Cs $6P_{3/2}$ level, obtained with the fast-beam laser [1] and level-crossing [7] methods, have accuracies of 0.9% and 0.7%, respectively, but differ from each other by $\sim 2.1\%$. Given the expected improvement in theory and the fact that the experimental errors are dominated by systematics, an alternative, high-precision method for measuring lifetimes is necessary. In this paper we use such an alternative method, time-correlated single-photon counting [16], to measure of the lifetimes of the $6p\,^2P_{1/2}$ and $6p\,^2P_{3/2}$ states in Cs. (Hereafter these states are referred to as $6P_{1/2}$ and $6P_{3/2}$.)

To date, the lifetime measurement method which has claimed the highest accuracy (0.15%) [10] has been the fast-beam laser method, where a fast-beam of atoms ($v/c \approx 0.1\%$) is selectively excited with a perpendicularly crossed laser beam to provide a $t=0$ point. The decay of the fluorescence is monitored as a function of distance downstream. The measured decay length is then transformed into a decay time by determination of the atom beam velocity. In contrast, in the single-photon counting technique, a fast pulse from a laser selectively excites the state of interest at $t=0$, starting a clock which is stopped by the arrival of a fluorescence photon. The measured time interval is binned and the sequence is repeated until the required statistics are attained. Because of the very high repetition rates now available from mode-locked laser systems, excellent statistics can be acquired rapidly. Thus, as in the fast-beam laser method, the final accuracy is determined by systematics. Here we demonstrate the capability of the single-photon counting technique to measure nanosecond lifetimes with accuracies at the 0.2–0.3 % level. Improvements to the method should enable lifetime measurements with accuracies $\approx 0.1\%$.

II. EXPERIMENT

The experiment was performed using the apparatus shown in Fig. 1. Briefly a short, linearly polarized laser pulse, resonant with the transition of interest $6S_{1/2}$-$6P_{1/2}$ ($6P_{3/2}$) at 895 nm (852 nm), excites Cs atoms in a well-collimated thermal atomic beam. In contrast to the fast-beam laser method, flight-from-view problems are negligible at these low velocities, since a Cs atom travels only 0.1 mm in ~ 10 lifetimes, corresponding to a change in the solid angle collected of $\sim 4\times 10^{-7}$. Fluorescence is detected at right angles to both the electric-field polarization axis of the laser and the laser propagation direction by a red-sensitive photomultiplier tube. Fluorescence photons pass through a polarizer, lens, filter, and slit before reaching the photomultiplier tube. The combined collection/detection efficiency is estimated to be $\approx 1\times 10^{-5}$. As is usual for high repetition rate sources, the counting electronics are operated in time-reversed mode in order to eliminate dead time due to reset of the time-to-amplitude converter (TAC). Therefore, the start pulse was provided by the arrival of a fluorescence photon that was processed through a constant-fraction discriminator. The stop pulse was provided by a fast photodiode which sampled a portion of the excitation pulse. The output of the TAC was binned by a multichannel analyzer (MCA) in conjunction with a personal computer.

Since we expected the experiment to be dominated by systematic errors, the atomic beam apparatus was designed to minimize these effects. In particular, radiation trapping was a major concern. In order to minimize this effect (and other density-dependent effects, i.e., collisions) the Cs atomic beam was well collimated at the interaction region and an extensive system of liquid-nitrogen-cooled baffles (not shown in Fig. 1) was employed to scavenge background Cs. In addition, fluorescence path limiters were placed inside the atomic beam chamber along the detection line of sight. The Cs beam effuses from a 0.17-mm-diam aperture, passes through a cooled aperture whose outer diameter was intentionally designed to capture and thereby eliminate most of the off-axis Cs beam, and is collimated with a 2-mm aperture placed just before the laser interaction region. A cryogenically cooled beam catcher was placed after the in-

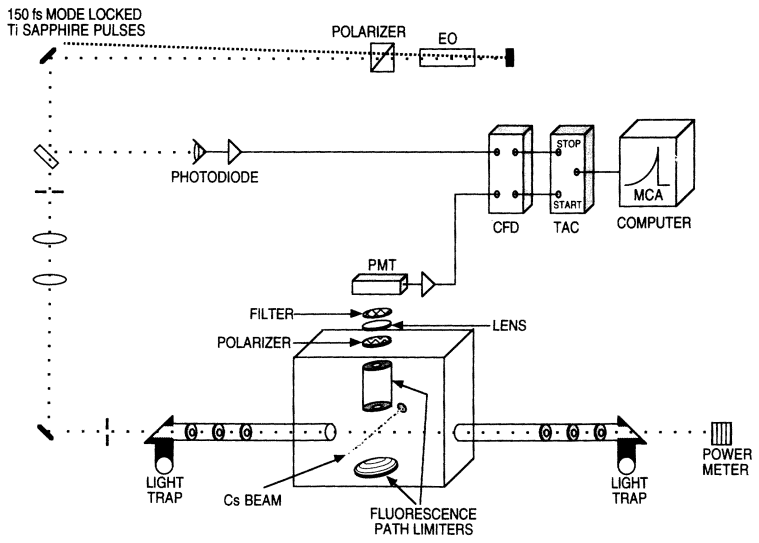

FIG. 1. A schematic of the experimental arrangement. EO is an electro-optic modulator, CFD is a constant-fraction discriminator, TAC is a time-to-amplitude converter, PMT is a photomultiplier tube, and MCA is a multichannel analyzer. See text for a detailed description.

teraction region in order to further reduce the Cs background. Based upon temperature measurements of the oven ($T_{oven}=340$ K) and nozzle, the Cs number density in the interaction region was nominally $\approx 1.5\times 10^{6}$ cm^{-3}. The true test of radiation trapping is the comparison of measured lifetimes at low and high density. These measurements were made with high statistics for the nominal low density cited above and a density approximately five times greater. The chamber background pressure was maintained at 2×10^{-7} Torr. Zeeman quantum beats were also of concern. The magnetic field in the interaction region was measured with a Hall probe to be ≈ 0.6 G with an orientation $\sim 9°$ from the electric-field polarization axis of the laser.

A commercial Ar^{+}-pumped, self-mode-locked Ti:sapphire laser was used to provide excitation pulses ($\Delta t \approx 150$ fs) at a repetition rate of ~ 76 MHz. Since this gives a period between pulses of 13.2 ns and the lifetimes of interest are ~ 30 ns, pulse selection was required. The Ti:sapphire laser was passively mode locked; therefore the pulse selection was accomplished external to the laser cavity by double passing [17] the pulses through an electro-optic modulator (EO) as shown in Fig. 1. The double-pass geometry was necessary to reduce the leakage of unwanted pulses (hereafter called afterpulses) to an acceptable level. The amplitude of the afterpulses in a single-pass geometry was measured to be $\sim 1\%$ and $\sim 0.2\%$ in double pass. For measurement of the $6P_{1/2}$ ($6P_{3/2}$) lifetimes 1 out of every 17 (15) pulses was selected, yielding ~ 20 mW of laser power in the atomic beam chamber.

The characteristics of the Ti:sapphire laser necessitated careful experimental design. The spectral bandwidth of the laser pulses (≈ 10 nm) is so large that $>99.9\%$ of the light is not resonant with the transition, leading to accentuated scattered light problems. Scattered light was decreased to the background level by the use of (1) long baffle arms with graded apertures, (2) light traps with windows at Brewster's angle on both the entrance and exit, and (3) a blackened atomic beam chamber. In addition, the large spectral bandwidth induces the coherent excitation of several hyperfine levels ($F'=2,3,4,5$) in the excited $6p\ ^2P_{3/2}$ state leading to the observation of hyperfine quantum beats [18]. In order to eliminate the hyperfine quantum beats, a linear polarizer was placed in the fluorescence detection stack at the "magic angle" (54.7°) with respect to the laser polarization direction to null the out-of-phase beating of the π and σ components of the radiation [19], as shown in Fig. 2.

A thorough understanding of the instrument function, i.e., the response of the detection system to a δ-function input, is also critical for high-precision results since the actual observed wave form is the convolution of the instrument function with an exponential decay. In this case the instrument function assumes greater importance because the extinction of the afterpulses is not complete. The instrument function was measured by two methods. The first involved rotating a pin point to the interaction region *in situ* (i.e., under the experimental running conditions) in order to scatter laser light into the detection system. This was an imperfect method since the afterpulse distribution had spatial variations due to the finite spot size in the EO. However, the pin scattering did serve as an excellent monitor for EO stability during the course of the experiment as well as a method for time calibration. The second method used to map the instrument function produced a true spatial average of the laser profile by Rayleigh scattering from air and the smoke generated from a dry ice-water mixture. It should be noted that both these methods of characterizing the afterpulse distribution have much greater dynamic range than simply measuring the output of the fast photodiode on an oscilloscope, where no afterpulses are visible. In addition, the use of a squirrel-cage style (side-on) photomultiplier tube (PMT) has the advantage that the spurious PMT afterpulse observed in end-on tubes is absent [16,17]. Here we note that the full width at half maximum of the PMT response to a δ-function input is ≈ 1.5 ns, well below the nominal lifetime of 35 ns (30 ns) for the $6P_{1/2}$ ($6P_{3/2}$) state.

The time calibration was mapped directly on the MCA by the afterpulses. The laser repetition rate was measured with a commercial frequency counter, which has an

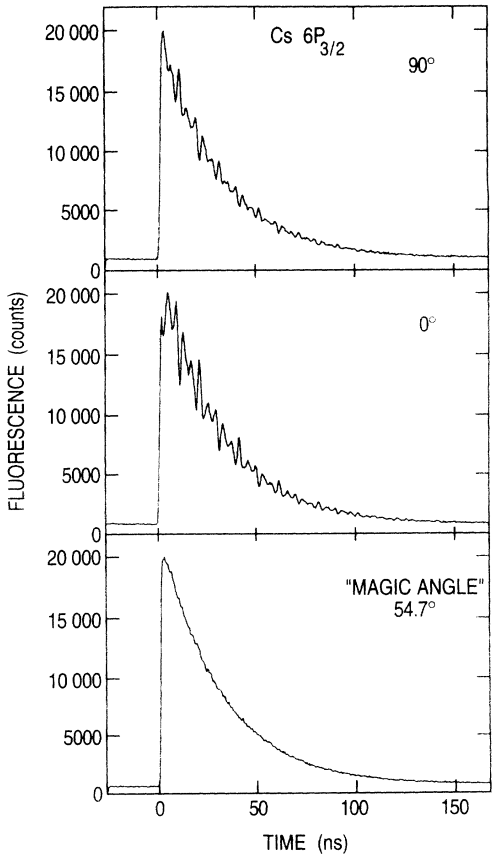

FIG. 2. Elimination of hyperfine quantum beats from fluorescence from the Cs $6P_{3/2}$ state. Top, middle, and lower panels show fluorescence from the $6P_{3/2}$ state with the detection polarizer oriented at 90°, 0°, and 54.7°, respectively, with respect to the electric-field polarization vector of the laser. 54.7° corresponds to the "magic angle" where $3\cos^2\theta - 1 = 0$.

accuracy of 10^{-7}. Therefore, any nonlinearities in the time scale were measured directly on the entire TAC-MCA system. Nonlinearities in the y scale of the TAC-MCA system were determined by counting random events (induced by scattering the output of a flashlight into the detection system) while maintaining the stop rate from the photodiode. Nonlinearities in the y scale could be induced by rf pickup from, say, the voltage pulse applied to the EO. Extensive shielding of the EO, EO power supply, and a low-pass filter placed directly at the high voltage input to the PMT substantially reduced these effects.

A typical experimental run of acquiring a Cs fluorescence decay at a signal rate of $\sim$2.5 kHz (4.0 kHz) with a laser repetition rate of 4.4 MHz (5.0 MHz) for the $6P_{1/2}$ ($6P_{3/2}$) levels to a peak of 10 000 or 20 000 counts in a particular channel required $\sim$5–10 min. The background rate, due entirely to dark counts, was typically 400 Hz, distributed uniformly among all channels. The decays were recorded out to $\sim 6\tau$. Interspersed between accumulations of Cs fluorescence decay data, we measured (1) laser-off resonance signals (to monitor scattered light), (2) pin scattering signals (to monitor afterpulse amplitude), and (3) "flashlight" scattering (to monitor rf pickup). For the $6P_{3/2}$ level, a total of 68 runs were taken at "low" density and about half the statistical precision was acquired in 20 runs at "high" density. For the $6P_{1/2}$ level, 30 runs were taken at "low" density and 13 runs at "high" density. The linear polarizer in the detection stack was removed and replaced with an aperture of equal size for the $6P_{1/2}$ runs since no hyperfine quantum beats are expected in this case.

III. RESULTS AND ANALYSIS

The observed wave forms were fit to a single exponential decay plus background using a nonlinear least-squares algorithm. Although this was not the optimal method of analysis, which would have been a deconvolution of the instrument function from the observed decay, we decided on this approach because the instrumental response measured during the experiment was not the appropriate spatially averaged response. However, we note that an analysis by forward convolution of the proper instrument function (acquired the day after the Cs decay curves using Rayleigh scattering as previously described) with an exponential decay yielded the same value as the simple analysis of the decay with a starting point $\approx$70% of the peak for the $6P_{1/2}$ data. Furthermore, by modeling the convolution of an instrumental response that has a train of equal fractional amplitude A afterpulses with a pure exponential decay, it was found that the simple analysis yielded the lifetime correct to within $A/10$. Thus, for our average fractional amplitude of afterpulses, 0.2%, the simple analysis would yield a lifetime in error by only 0.02%, a much smaller uncertainty than contributed by other factors.

In Fig. 3 an example of an instrument function, decay of the $6P_{3/2}$ state, and residuals with statistical error bars from a fit to a single exponential decay plus background are shown in the top, middle, and bottom panels, respectively. In this case, the instrument function was obtained by pin scattering and therefore does not represent a true spatially averaged response. The hyperfine quantum beats have been eliminated from the decay by orientation of the polarizer in the detection stack at 54.7° with respect to the laser polarization axis. The reduced χ^2 of the individual fits was typically 1.1, well within the range expected for good single-photon counting data with slightly non-Poissonian distributed noise (0.8–1.2) [16].

In Fig. 4 a similar set of data is shown for the $6P_{1/2}$ state. In this case, the instrument function was obtained by Rayleigh scattering. Note that the amplitude of the afterpulses is much more constant in this spatially averaged case than in the pin scattered data of Fig. 3. The average amplitude of the afterpulses was $\approx$0.2%, consistent with residuals resulting from a fit to the overall summed data.

For the $6P_{1/2}$ and $6P_{3/2}$ levels the mean fitted lifetimes at low density were 34.75 and 30.39 ns, respectively. The standard deviations of the mean for all the low-density measurements were 0.1% (0.14%) for $6P_{1/2}$ ($6P_{3/2}$). The

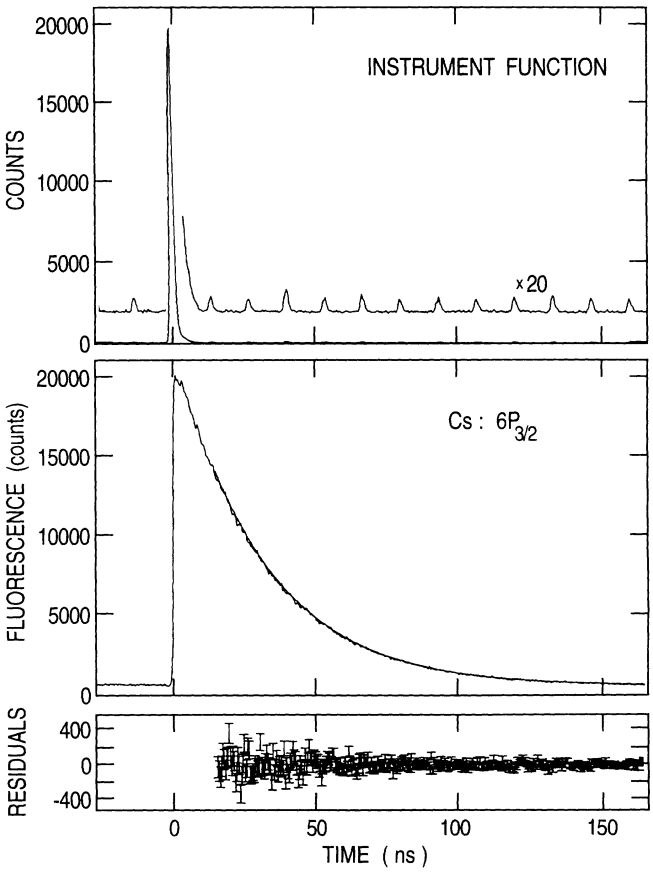

FIG. 3. Top panel shows an instrument function taken by pin scattering with the laser tuned to the $6S_{1/2}$-$6P_{3/2}$ transition at 852 nm. Middle panel shows fluorescence from the $6P_{3/2}$ state with the hfs quantum beats nulled as shown in Fig. 2, as well as the fit to a single exponential plus background. Lower panel shows the residuals from the fit.

values above correspond to a fit of the decay starting at ~70% of the peak, or ~11 ns after the peak (well after any tail of a PMT response to a δ-function input). For any specific starting point of the data analysis, a fit of the summed data yielded a lifetime consistent with the mean of the individual fits to 0.02%. The statistical uncertainties are small relative to the systematic uncertainties, which are shown in Table I and will be discussed next.

The absolute scale for the time calibration was set by counting the repetition rate of the laser excitation pulses as described above. Nonlinearities in the time scale were then determined by fitting the peak positions of the afterpulses to a second-order polynomial. The nominal afterpulse amplitude of 0.2% was easily enhanced for time calibration by detuning the EO voltage from its half-wave value to allow greater leakage of afterpulses. The fit revealed no nonlinear term in the time scale at a level of $\sim 10^{-4}$. The linear term varied no more than 0.02% over many days, and we take this as the uncertainty in the time calibration.

The nonlinearities in the y scale were checked by counting random events as described above. The accumulated result should be a constant over all channels if there is no systematic trend that varies the effective bin width of the MCA-TAC combination. Although the accumulated counts showed some nonstatistical deviations (most likely originating from residual rf pickup) at the 0.5% level, the data are fit by a constant with linear and quadratic terms that do not differ from zero at the 2×10^{-5} level. Analyzing data grouped in 10 and 20 channel bins again reveals scatter, but no systematic trends with channel position. The standard deviation in the mean value of the constant is 0.05% and we take twice this value to the largest possible systematic uncertainty.

TABLE I. Single-photon counting error budget for the lifetimes of the $6p\ ^2P_{1/2}$ and $6p\ ^2P_{3/2}$ states in Cs.

Systematic	Error (%) $6P_{1/2}$	$6P_{3/2}$
Time calibration	±0.02	±0.02
TAC-MCA nonlinearity	±0.10	±0.10
Pulse pileup	±0.03	±0.03
Afterpulse amplitude	±0.02	±0.02
Radiation trapping	±0.06	±0.06
Hyperfine quantum beats		±0.07
Zeeman quantum beats		+0.13±0.10
Truncation error	±0.15	±0.21
Total systematic	±0.19	+0.13±0.27
Statistical	±0.10	±0.14
Sum in quadrature	±0.22	+0.13±0.31

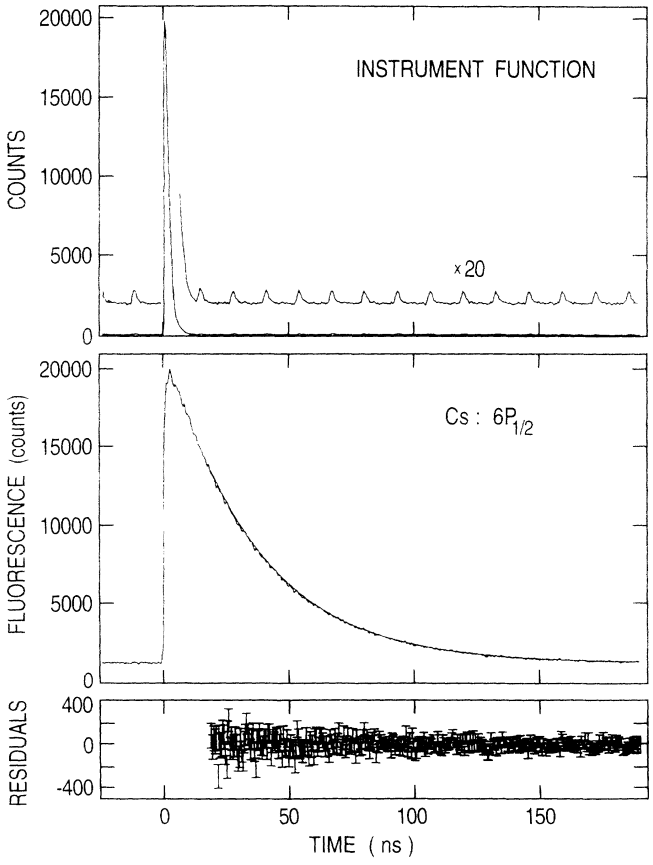

FIG. 4. Top panel shows an instrument function taken by Rayleigh scattering from air with the laser tuned to the $6S_{1/2}$-$6P_{1/2}$ transition at 895 nm. Middle panel shows fluorescence from the $6P_{1/2}$ state, as well as the fit to a single exponential plus background. Lower panel shows the residuals from the fit.

Pulse pileup in the MCA results from the statistics generated by the counting process and can be analytically corrected [16]. That is, due to the fact that the TAC is stopped only once during an excitation cycle, counts at early stop times are preferentially counted leading to a systematic correction in the fitted decay. The effect is obviously more pronounced when the detection rate is a significant fraction of the excitation rate. We therefore kept the fraction of detected events below $\frac{1}{1000}$ of the excitation events. The analytical correction for the true number of counts N_A in the ith channel is given by

$$N_A = \frac{N_i}{1-\frac{1}{N_E}\sum_{j=1}^{i-1} N_j},$$

where N_E is the number of excitation cycles and N_i is the observed number of counts in channel i. With this correction, we find that, for data analysis starting from 70% of the peak height, the fitted lifetime decreases by 0.03%.

The extent of radiation trapping (and other collisional effects) were evaluated by varying the Cs beam density by a factor of ~5 for both the $6P_{1/2}$ and $6P_{3/2}$ levels. This was accomplished by varying the Cs oven temperature and not by any changes in experimental geometry. The change in the lifetime between high and low density was

$\sim 0.29\%$ for both levels. Dividing by 5 (a conservative estimate) for a linear extrapolation to zero density yields a systematic error of 0.06% for radiation trapping–Cs-Cs collisions, which is statistically insignificant. This is consistent with the estimated reabsorption probability for the density and column length along the detection path (1.5×10^6 Cs cm^{-3}, 0.24 cm, $\sigma_{abs}\approx10^{-10}$ cm^2). Collisions with background gas are not expected to be important at these pressures. The quenching cross sections for the lowest excited p states in Rb by N_2 [20] are ≈ 50 Å^2. For Cs-N_2 collisions with a relative velocity of $\sim 4\times10^4$ cm/s and a background density of N_2 of $7\times10^9/cm^3$, a quenching cross section of $\sim 10^7$ Å^2 would be required to change the lifetime by 1%. Thus these effects are considered negligible.

Hyperfine quantum beats are present only in the decay of the $6P_{3/2}$ level. The magnitude of their effect was estimated as follows. For decays with the detection polarizer oriented at 0° or 90°, the quantum beats due to hfs are clearly apparent, as shown in Fig. 2. It is also clear that the lifetime will depend on the range of data included in the fitting procedure, i.e., whether one begins fitting on a peak or a valley. These variations can be quite large, with a peak-to-valley amplitude change of ~ 3–5%. Therefore, it was considered best to compare a weighted average of the fitted lifetimes over a large fit range with the same quantity for the decays free from hfs quantum beats. In this comparison, it was found that the $\sigma(\pi)$ radiative lifetime differed from the quantum beat free lifetime by ~ 0.1–0.2%. Unfortunately, the statistical significance of this result is at the 1.2% level due to the small amount of data taken at the 0° and 90° detection angles. Since these lifetime variations are due to the maximum quantum beat size and they are attenuated by at least 50 times due to magic angle orientation of the detection polarizer ($\sim$500:1 extinction at 852 nm), a value of 0.07% is assigned to the systematic uncertainty due to hfs quantum beats [corresponding both to $(3\times1.2)\%/50$ and the peak-to-valley change $\sim 4\%/50$].

The systematic effects of Zeeman quantum beats in the decays can be calculated for the Cs system [21,22]. These are particularly insidiuous because at the low fields (0.6 G) present in the experiment, there are no observable beats. For an orientation of the B field coincident with the laser electric-field polarization axis, $\Delta m = 0$ selection rules rigorously prohibit the generation of Zeeman quantum beats. However, the B field in this experiment was actually tipped at $\sim 9°$ from the laser polarization axis toward the detection axis. This enabled a small admixture (2.7%) of σ excitation and resulting quantum beats to be present in the decay. A simulation of this was done, including convolution with an instrument function, to yield a decay which could be fitted by the single exponential plus background. The fitted lifetime for the $6P_{3/2}$ state is found to be 0.13% shorter than the decay free from quantum beats with an estimated uncertainty of 0.10% arising from the combination of an allowed $\pm 10°$ variation in the orientation and a $\pm 15\%$ variation in the B-field strength. We make this 0.13% correction for this state as shown in Table I. For the $6P_{1/2}$ state, the Zeeman quantum beat effects are negligible.

Finally, the largest systematic error found is the variation of the lifetime with the starting point of the fit, termed truncation error. By assessing effects through the convolution of instrument functions with model decays, it was determined that this systematic was due to the *variation* in the afterpulse amplitudes. As discussed earlier, the actual magnitude of the afterpulses results in only a small distortion of the fitted lifetimes (change of 0.02% for 0.2% afterpulse). However, it is the variation in the afterpulse amplitude that causes this much larger error. These variations in afterpulse amplitude could be caused by, e.g., electrical reflections in the EO transmission line, resulting in some variation in the voltage applied to the EO, and hence in the transmission of the afterpulse. The magnitude of the afterpulse variation is estimated to be at most 40%, which in turn leads to an error in the fitted lifetime of 0.23% when the starting point of the fit is at $\sim 70\%$ of the peak. (A more likely value for the magnitude of the afterpulse variation is $\sim 20\%$, based upon the Rayleigh scattering instrument function data, as shown in the top panel of Fig. 4.) As one would expect, the effect of the variation in afterpulse magnitude increases as the starting point is moved out in time, whereas the tail of the PMT response is enhanced at early start times. For the $6P_{1/2}$ data the observed variation in lifetime as a function of fit range was $\pm 0.15\%$, for starting points ranging between 80% and 50% of the maximum (9–28 ns after the pulse). The weighted average of these fitted lifetimes is reported for the $6P_{1/2}$ level. (The $6P_{1/2}$ data were also analyzed using the Rayleigh scattering instrument function in a forward convolution with a single exponential decay. In this analysis, there was no systematic variation of the fitted lifetime starting from 90% to 50% of the peak.) For the $6P_{3/2}$ data, the observed changes in lifetime over the same fit range were $\pm 0.31\%$, $\pm 0.12\%$, and $\pm 0.09\%$ for cumulative runs on three different days, with EO realignments interspersed. As in the previous case, for the $6P_{3/2}$ data the weighted average of data with starting points between $\sim 80\%$ and 50% of the maximum is reported as the actual lifetime and a truncation error of 0.21% was assigned.

IV. COMPARISON WITH MBPT

The values obtained for the $6P_{1/2}$ and $6P_{3/2}$ lifetimes are shown in Table II, along with the values derived from

TABLE II. Comparison of selected experimental and theoretical lifetimes for $6P_{1/2}$ and $6P_{3/2}$ levels in Cs.

Experimental method	Lifetime (ns) $6P_{1/2}$	$6P_{3/2}$
Single-photon counting (this work)	34.75(7)	30.41(10)
Fast-beam laser [26]	34.934(94)	30.499(70)
Fast-beam laser [1]		30.55(27)
Level crossing [7]		29.9(2)
Theoretical MBPT calculations		
Blundell, Johnson, and Sapirstein [3]	34.51	30.13
Dzuba *et al.* [4]	34.92	30.49

the two *ab initio* MBPT calculations performed by Blundell, Johnson, and Sapirstein [3] and Dzuba *et al.* [4]. For the theoretical values, *ab initio* matrix elements and experimental energies are used to compute the lifetimes. In addition, we include the previous most accurate results ($<1\%$) derived from fast-beam laser and level-crossing experiments for comparison. A more complete survey of other experimental results can be found in Ref. [1]. As can be seen from the table, the lifetimes measured in this work are consistently longer than the values obtained by Blundell, Johnson, and Sapirstein by $\sim 0.7-0.9\%$. This leads to a disagreement between experiment and Blundell, Johnson, and Sapirstein's theoretical dipole matrix elements of $\sim 0.3-0.5\%$, corresponding to the estimated level of uncertainty in the calculation 0.5%. Although the significance is diminished by the theoretical uncertainty, it should be noted that the same trend is found in the lighter alkali-metal atoms, where the measured lifetimes are consistently longer than those calculated [2]. It is unfortunate that only Blundell, Johnson, Sapirstein, and co-workers have performed MBPT calculations on both the light [11,12] and heavy [3] alkali-metal atoms, so that comparisons between few- and many-electron systems are limited to their results. In contrast to those from Blundell, Johnson, and Sapirstein, the calculations of Dzuba *et al.* are longer than the present results and are in agreement at the few tenths of a percent level.

A comparison to other sub-1% experimental results is shown also in Table II. The present single-photon counting lifetimes appear to be consistently faster than the fast-beam laser results and slower than the level crossing results, but not by an amount that is statistically worrisome, i.e., $\leq 2\sigma_{\text{combined}}$.

Not shown in Table II is the comparison of relative oscillator strengths obtained from these measurements. Our value for the ratio $f(6P_{3/2})/f(6P_{1/2})$ is 2.075(8). This is in good agreement with the previous most accurate study of Shabanova, Monakov, and Khlyustalov [23], who obtain a value of 2.078(12), as well as an earlier semiempirical calculation by Norcross [24], who obtains 2.08.

V. DISCUSSION AND CONCLUSIONS

We have demonstrated the capability of the single-photon counting technique to measure lifetimes in the nanosecond regime to an accuracy of a few tenths of a percent. These values are the most accurate lifetime measurements of the first excited p states in Cs. The accuracy of our present results is not limited by factors which are intrinsic to the technique, but rather due to the particular implementation. Complete removal of the afterpulse train (and hence variations in afterpulse amplitude that lead to the largest systematic uncertainty, truncation error) can be accomplished by cavity dumping the laser rather than using an external EO modulator. Alternatively, an *in situ* measurement of the proper instrument function (in our case, the spatially averaged Rayleigh scattering) would also eliminate the truncation error and allow data treatment by convolution. This would have the added advantage of permitting the analysis of fast decays in which the lifetime approaches the instrument function width. A more careful alignment or nulling of the magnetic field that provides the quantization axis can essentially eliminate effects due to Zeeman quantum beats. In addition, performing the experiment on a single ion in a trap can eliminate the effects due to radiation trapping and hyperfine quantum beats (with judicious choice of isotope). The feasibility of such experiments has been demonstrated in the alkali-metal-like Ba^+ ion [25]. With these improvements, one an expect lifetimes to be measured at the $\sim 0.1\%$ level in the near future using single-photon counting.

The single-photon counting technique can also be easily extended to measure higher-lying excited states in various alkali-metal atoms. In Cs it is these higher-lying levels, i.e., $7P_{1/2}$ and $7P_{3/2}$, that exhibit much greater discrepancy with MBPT theory. Since the single-photon counting technique uses high-repetition-rate pulsed lasers, frequency doubling to reach the appropriate wavelengths is not difficult.

In summary, the lifetimes of the $6P_{1/2}$ and $6P_{3/2}$ states in Cs have been measured by the single-photon counting technique with accuracies at the $0.2-0.3\%$ level. The lifetimes are in agreement with those derived from *ab initio* MBPT calculations of the dipole matrix elements [3,4] in combination with the experimental values for the transition energies [27] at the sub-1% level. This confirms the accuracy of the *ab initio* calculations of the dipole matrix elements at the 0.5% level, in agreement with the estimated theoretical uncertainty. The trends observed in the lighter alkali-metal atoms, i.e., measured lifetimes longer than those from Blundell, Johnson, and Sapirstein's MBPT calculations, is also observed for Cs, at approximately the same level.

ACKNOWLEDGMENTS

L.Y., W.T.H., and S.J.S. thank the Joint Institute for Laboratory Astrophysics (JILA) for the support of the Visiting Fellow Program, which made this experiment possible. We also thank J. Hall, A. Phelps, and the JILA electronics shop for the loan of equipment and useful suggestions. H. Green and P. Smith were instrumental in the construction of the atomic beam apparatus. S.J.S. thanks D. Cho for helpful discussions concerning Cs beam operation. L.Y. thanks G. R. Fleming, S. Rosenthal, and C. Kunasz for helpful discussions. C.E.T. was supported by the Luce Foundation and the University of Notre Dame. This research was supported by the National Science Foundation and the U.S. Department of Energy, Office of Basic Energy Science under Contract No. W-31-109-ENG-38.

[1] C. E. Tanner, A. E. Livingston, R. J. Rafac, F. G. Serpa, K. W. Kukla, H. G. Berry, L. Young, and C. A. Kurtz, Phys. Rev. Lett. **69**, 2765 (1992).
[2] J. Jin and D. A. Church, Phys. Rev. Lett. **70**, 3213 (1993).
[3] S. A. Blundell, W. R. Johnson, and J. Sapirstein, Phys. Rev. A **43**, 3407 (1991).
[4] V. A. Dzuba, V. V. Flambaum, A. Ya. Kraftmakher, and O. P. Sushkov, Phys. Lett. A **142**, 373 (1989).
[5] M. C. Noecker, B. P. Masterson, and C. E. Wieman, Phys. Rev. Lett. **61**, 310 (1988).
[6] S. A. Blundell, W. R. Johnson, and J. Sapirstein, Phys. Rev. Lett. **65**, 1411 (1990).
[7] S. Rydberg and S. Svanberg, Phys. Scr. **5**, 209 (1972); S. Svanberg and S. Rydberg, Z. Phys. **227**, 216 (1969).
[8] C. E. Tanner and C. E. Wieman, Phys. Rev. A **38**, 162 (1988).
[9] L. R. Hunter, D. Krause, Jr., K. E. Miller, D. J. Berkeland, and M. G. Boshier, Opt. Commun. **94**, 210 (1992).
[10] A. Gaupp, P. Kuske, and H. J. Andrä, Phys. Rev. A **26**, 3351 (1982).
[11] S. A. Blundell, W. R. Johnson, Z. W. Liu, and J. Sapirstein, Phys. Rev. A **40**, 2233 (1989).
[12] C. Guet, S. A. Blundell, and W. R. Johnson, Phys. Lett. A **143**, 384 (1990).
[13] J. Carlsson, Z. Phys. D **9**, 147 (1988).
[14] J. Carlsson and L. Sturesson, Z. Phys. D **14**, 281 (1989).
[15] S. A. Blundell, J. Sapirstein, and W. R. Johnson, Phys. Rev. D **45**, 1602 (1992).
[16] D. V. O'Connor and D. Phillips, *Time Correlated Single Photon Counting* (Academic, London, 1984).
[17] D. Bebelaar, Rev. Sci. Instrum. **57**, 1116 (1986).
[18] S. Haroche, J. A. Paisner, and A. L. Schawlow, Phys. Rev. Lett. **30**, 948 (1973).
[19] J. S. Deech, R. Luypaert, and G. W. Series, J. Phys. B **8**, 1406 (1975).
[20] W. Happer, Rev. Mod. Phys. **44**, 169 (1972).
[21] M. P. Silverman, S. Haroche, and M. Gross, Phys. Rev. A **18**, 1517 (1978).
[22] P. J. Brucat and R. N. Zare, J. Chem. Phys. **78**, 100 (1983).
[23] L. N. Shabanova, Yu. N. Monakov, and A. N. Khlyustalov, Opt. Spektrosk. **47**, 3 (1979) [Opt. Spectrosc. (USSR) **47**, 1 (1979)].
[24] D. W. Norcross, Phys. Rev. A **7**, 606 (1973).
[25] R. Devoe (private communication).
[26] R. Rafac *et al.* (unpublished).
[27] C. E. Moore, *Atomic Energy Levels as Derived from the Analyses of Optical Spectra,* Natl. Bur. Stand. Ref. Data Ser., Natl. Bur. Stand. (U.S.) Circ. No. 35 (U.S. GPO, Washington, DC, 1971), Vol. III.

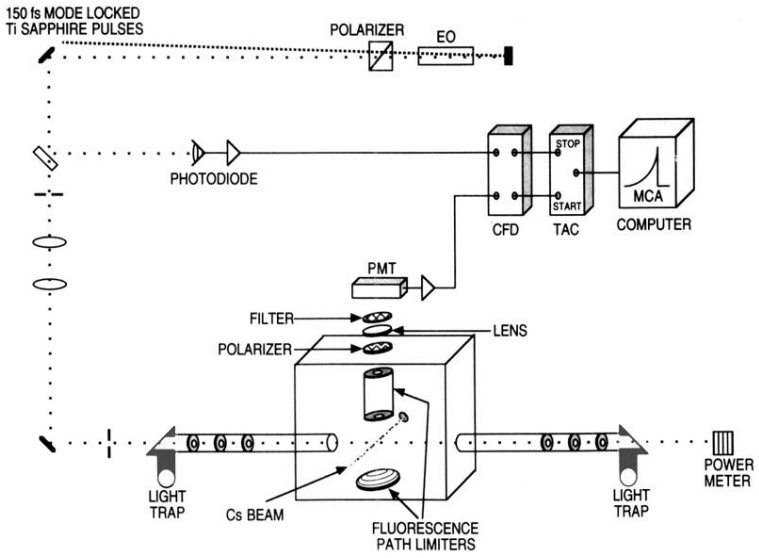

FIG. 1. A schematic of the experimental arrangement. EO is an electro-optic modulator, CFD is a constant-fraction discriminator, TAC is a time-to-amplitude converter, PMT is a photomultiplier tube, and MCA is a multichannel analyzer. See text for a detailed description.